Analyst

Accepted Manuscript

ROYAL SOCIETY OF CHEMISTRY

www.rsc.org/analyst

Graphical Abstract

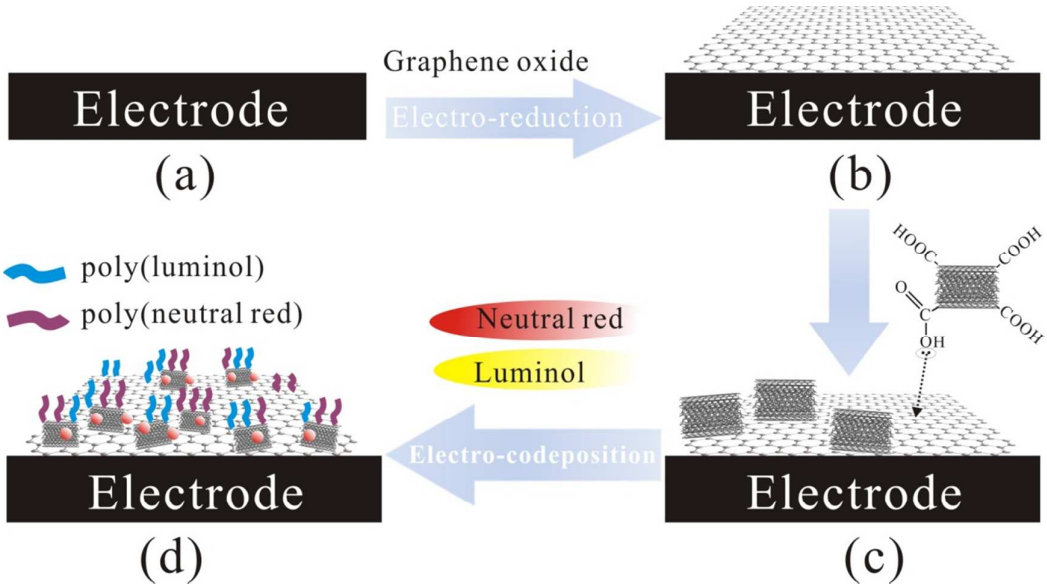

Illustration of electro-codeposition of poly(luminol) and poly(neutral red) hybrid films using high conductive and steric MWCNT-GO as a template.

Cite this: DOI: 10.1039/c0xx00000x

www.rsc.org/xxxxxx

ARTICLE TYPE

A highly sensitive NADH sensor based on mycelium-like nanocomposite using graphene oxide and multi-walled carbon nanotubes to coimmobilize poly(luminol) and poly(neutral red) hybrid films

Kuo Chiang Lin, Szu Yu Lai and Shen Ming Chen*

Received (in XXX, XXX) Xth XXXXXXXXX 20XX, Accepted Xth XXXXXXXXX 20XX
DOI: 10.1039/b000000x

Hybridization of poly(luminol) (PLM) and poly(neutral red) (PNR) has been successfully performed and further enhanced by a conductive and steric hybrid nanotemplate using graphene oxide (GO) and multi-walled carbon nanotubes (MWCNT). Morphology of PLM-PNR-MWCNT-GO mycelium-like nanocomposite is studied by SEM and AFM and it is electroactive, pH-dependent, and stable in the electrochemical system. It shows eletrocatalytic activity to NADH with high current response and low overpotential. By amperometry, it shows a high sensitivity of 288.9 μA mM^{-1} cm^{-2} to NADH ($E_{app.}$ = +0.1 V). Linearity is estimated in a concentration range of 1.33×10^{-8}–1.95×10^{-4} M with a detection limit of 1.33×10^{-8} M (S/N = 3). Particularly, it also shows another linear range of 2.08×10^{-4}–5.81×10^{-4} M with a sensitivity of 151.3 μA mM^{-1} cm^{-2}. Hybridization and activity of PLM and PNR can be effectively enhanced by MWCNT and GO, performing an active hybrid nanocomposite for determination of NADH.

1. Introduction

Reduced *β*-nicotinamide adenine dinucleotide (NADH) and its oxidized form, NAD^+, are very important coenzymes that play an important role in the energy production/consumption of cells of all living organisms. NADH participates in a variety of enzymatic reactions via more than 300 dehydrogenases.[1] Many studies have focused on the fundamental scientific applications of the NADH reaction. Numerous analytical methods have been proposed for NADH detection, including colorimetry,[2] fluorescence,[3] enzymatic assay,[4] high-performance liquid chromatography,[5] electrospray ionization mass spectrometry,[6] capillary electrophoresis,[7] and electrochemical assay.[8,9] It has received considerable interest due to its very important role as a cofactor in a whole diversity of dehydrogenase-based bioelectrochemical devices such as biosensors, biofuel cells, and bioreactors.[10-12] However, direct oxidation of NADH at a conventional solid electrode is highly irreversible, requires large activation energy, and proceeds with coupled side reactions, poisoning the electrode surface.[13-15] In recent years, many nanomaterials, especially various carbon nanomaterials,[16-18] have been used widely to reduce the overpotential for NADH oxidation and minimize the surface contamination effect without the help of redox mediators.

Since two decades carbon nanotubes (CNTs) have been gaining popularity due to their unique properties such as electronic, metallic and structural characteristics.[19] CNTs have outstanding ability to mediate fast electron transfer kinetics for a wide range of electroactive species and show electrocatalytic activity towards biologically important compounds such as NADH and H_2O_2.[20,21] Recently, the fabrication of CNTs/conducting polymer composites has gained great interest as the CNTs can improve the electrical and mechanical properties of polymers[22,23] and it has been demonstrated that the obtained CNTs/conducting polymer possess properties of the individual components with a synergistic effect.[24-29] Particularly, CNTs might play a role as a template to immobilize conducting polymers especially for different conducting polymers hybridization.

Graphene oxide (GO) consists of a single atomic layer of sp^2-hybridized carbon atoms functionalized with mainly phenol, hydroxyl, and epoxide groups on the basal plane and ionizable carboxyl groups at the edges; it is obtained after treating graphite with strong oxidizers. GO can form stable single-layer aqueous dispersions due to the charge repulsion of the ionized edge acid groups. As a derivatized graphite nanomaterial, GO features a highly hydrophobic surface with non-oxidized polyaromatic nanographene domains on the basal plane. The abundance of highly conjugated structures on the surface of GO allows it to adhere readily to conjugated materials through π–π interactions, making GO function as a unique tethered 2D surfactant sheet.[31-35]

Recently, many studies have confirmed that GO is a good candidate for use as an advanced carbon material in electrochemical applications.[36-38] Because CNTs and GO exhibit many similar properties, while being structurally dissimilar, then on covalent preparation of rGO/CNT composites provides attractive building blocks for the development of nanocarbon materials with potentially improved conductivity and catalytic ability for electrochemical research.

Luminol (LM) has been widely used in chemiluminescence detection,[39] electrochemiluminescence,[40,41] as well as for immunoassays using a flow injection system and liquid

chromatography.[42,43] As the polyluminol (PLM) film modified on the working electrode, it provides a reversible redox couple involving electron transfer. Such as previous works, this modified electrode also can be applied to study the electrocatalytic properties of biological molecules[44] and the reversible $NADH/NAD^+$ redox system.[45] The electrocatalytic activity for NADH oxidation is improved using the hybrid composites of PLM and nanomaterials.[46]

In the present investigation, luminol (LM) a versatile chemical and neutral red (NR) a phenazine redox dye are proposed to co-immobilize on electrode surface because they have an amino group located on the heteroaromatic ring, makes them amenable to facilitate electropolymerization,[44,47,48] and their good activities also have been gradually disclosed in the literature.[44,46,48,49] The use of GO and MWCNT to improve the hybridization of conducting polymers and the electrocatalytic property is also studied.

In this work, a simple electrochemical synthesis of PLM and PNR hybrid film formation is studied with an active MWCNT-GO-electrode. The PLM-PNR-MWCN-GO hybrid nanocomposite can be easily prepared on electrode surface through electropolymerization of LM and NR monomers using suitable arrangement of MWCNT and GO as an active and steric template. The hybrid composites are electrochemically characterized and the electrocatalytic oxidation of NADH is also investigated.

2. Experimental

2.1 Reagents and materials

Nicotinamide adenine dinucleotide (NADH), luminol (LM), neutral red (NR), and multi-walled carbon nanotubes (MWCNT) were purchased from Sigma-Aldrich (USA) and were used as-received. All other chemicals (Merck) used were of analytical grade (99%). Double-distilled deionized water (> 18.1 MΩ cm^{-1}) was used to prepare all the solutions. All other reagents were of analytical grade and used without further purification. A pH 5.5 phosphate buffer solution (PBS) was prepared with 0.05 M Na_2HPO_4 and 0.05 M NaH_2PO_4 and adjusted to pH 5.5 by phosphoric acid.

2.2 Apparatus and measurements

The PLM-PNR-MWCNT-GO hybrid composite was characterized by cyclic voltammetry, UV–visible spectroscopy, SEM, AFM, and amperometry. A glassy carbon electrode (GCE) was purchased from Bioanalytical Systems (BAS) Inc., USA. All GCEs were used with diameter of 0.3 cm (exposed geometric surface area of A = 0.0707 cm^2) for all electrochemical techniques. Electrochemical experiments were completed by a CHI 1205a electrochemical workstation (CH Instruments, USA) with a conventional three-electrode setup containing a GCE, an Ag/AgCl (3 M KCl) electrode, and a platinum wire as working, reference, and counter electrode, respectively. The buffer solution was entirely deaerated using nitrogen gas atmosphere. The morphological characterization of composite films was examined by means of SEM (S-3000H, Hitachi) and AFM images were recorded with multimode scanning probe microscope (Being Nano-Instruments CSPM-4000, China). Indium tin oxide (ITO) substrates were used in morphological analysis for convenience.

2.3 Fabrication of PLM-PNR and PLM-PNR-MWCNT-GO modified electrodes

The electropolymerization of luminol (LM) and neutral red (NR) was carried out in pH 5.5 PBS containing 1.5×10^{-3} M LM and 1×10^{-4} M NR by consecutive cyclic voltammetry. Potential cycling was controlled in the potential range of -0.7 ~ +0.6 V with scan rate of 0.1 Vs^{-1} and 15 scan cycles. Both bare and MWCNT-GO modified electrodes were used to have the electropolymerization of LM and NR.

The MWCNT-GO modified electrode was prepared by two steps: firstly, the electrochemical reduction of graphene oxide (GO), then, the adsorption of MWCNT. GO-modified electrode was prepared in the procedures: firstly, the GO solution (0.5 mg ml^{-1}) was prepared in 0.5 M sulfuric acid, then, electrochemical reduction of GO was achieved by employing consecutive cyclic voltammetry in the potential range of 0 to -1.4 V (15 cycles, scan rate = 0.05 Vs^{-1}). All MWCNT were carboxylic functionalized and well-dispersed in PBS (1 mg ml^{-1}) with sonication for 10 minutes. By drop-casting, 10 µl of the solution was dropped on electrode surface and dried out in the oven at 40 ℃. Consequently, the MWCNT-GO modified electrode was transferred to have hybrid electropolymerization of LM and NR in pH 5.5 PBS containing 1.5×10^{-3} M LM and 1×10^{-4} M NR by consecutive cyclic voltammetry. After these procedures, the LM-PNR and PLM-PNR-MWCNT-GO modified electrodes were prepared to study.

3. Results and Discussion

3.1 Preparation and characterization of PLM-PNR-MWCNT-GO hybrid composite

Hybridization of PLM and PNR is studied due to their activities and easy electropolymerization of monomers. However, the electropolymerization of two kinds of monomers might suffer the difficulty of disorder of polymer chains. Fig. 1A shows the consecutive cyclic voltammogram of LM and NR electropolymerization using a bare GCE. Poor current development of redox peaks indicates that the hybrid electropolymerization of LM and NR is not perfect. In our strategy, MWCNT-GO was used as a conductive and steric substrate to enhance the hybrid electropolymerization of hetero-monomers (LM and NR) on the electrode surface. Fig. 1B shows the consecutive cyclic voltammogram of LM and NR electropolymerization using a MWCNT-GO/GCE. The cyclic voltammogram depicts significant current development of LM and NR electropolymerization at MWCNT-GO/GCE better than that of bare GCE. It exhibits three obvious redox couples with formal potential of $E^{0'}_1$ = -0.5 V, $E^{0'}_2$ = 0 V, $E^{0'}_3$ = +0.27 V, related to NR, PNR (Redox couple 1 and 2) and PLM (Redox couple 3), respectively. Good current development is recorded in the plot of peak current vs. scan cycle (inset of Fig. 1B). Both anodic and cathodic peak currents are increasing as the increase in the scan cycles. It indicates that MWCNT-GO can effectively enhance the hybrid electropolymerization of hetero-monomers (LM and NR). Considering the previous report,[50] a novel hybrid nanomaterial (GO–MWNT) was explored based on the self-assembly of multi-walled carbon nanotubes (MWNTs) and graphene oxide (GO), which can drive positively charged horse

radish peroxidise (HRP) immobilize onto GO–MWCNT by the electrostatic interaction. So that, the phenomenon indicates the conductive and steric MWCNT-GO structure can provide more active sites to load the positively charged PLM and PNR, avoiding disorder of polymer chains. One can conclude that the hybrid films formation of PLM and PNR can be improved by MWCNT-GO.

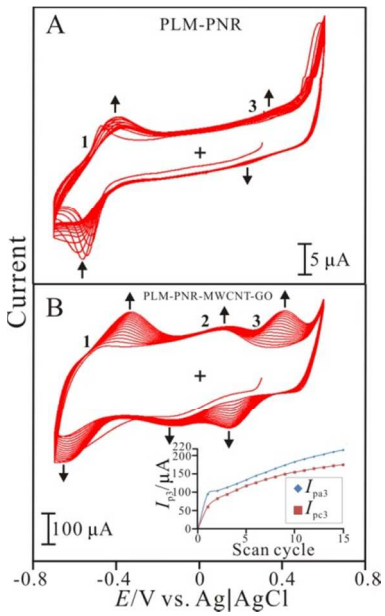

Fig. 1 Consecutive cyclic voltammograms (A) bare GCE and (B) MWCNT-GO/GCE examined in pH 5.5 PBS containing 1.5×10^{-3} M luminol and 1×10^{-4} M neutral red. Scan rate = 0.1 Vs^{-1}.

The experiment was designed to understand the spectra of these materials in the solution by UV-Visible spectroscopy. Fig. S1 shows the UV-Vis spectra of different materials and mixtures prepared in pH 7 PBS. The UV-Vis spectrum of GO shows absorption peak at 227 nm accompanied with a minor absorption peak at 300 nm. The spectrum of MWCNT shows absorption peak at 253 nm. The spectrum of their mixture exhibits absorption peaks at 239 nm and 300 nm resulted from the overlapping of GO and MWCNT spectra. NR shows absorption peaks at 276 nm and 528 nm while LM shows absorption peaks at 218 nm, 300 nm, and 347 nm. The spectrum of their mixture exhibits the absorption peaks (221 nm, 278 nm, 347 nm, and 531 nm) similar to their single spectrum. Furthermore, the spectrum of LM, NR, MWCNT, and GO mixture also shows absorption peaks at 221 nm, 278 nm, 347 nm, and 531 nm similar to their single spectrum. These phenomena indicate that these materials can be mixed stably to be a stable hybrid composite.

Different materials modified electrodes were prepared and studied by cyclic voltammetry. Fig. 2 shows the voltammograms of (a) PLM, (b) GO, (c) MWCNT, (d) PNR, and (e) PLM-PNR-MWCNT-GO modified electrodes. PLM shows a redox couple with formal potential of $E^{0'}$ = +0.27 V while PNR shows two redox couples of $E^{0'}$ = -0.52 V and $E^{0'}$ = +0.06 V. No obvious redox couples can be found in GO and MWCNT. It means that no electrochemical process for these species. PLM-PNR-MWCNT-GO shows significant redox couples estimated with formal potential of $E^{0'}_1$ = -0.51 V, $E^{0'}_2$ = 0 V, $E^{0'}_3$ = +0.26 V, related to NR, PNR (Redox couple 1 and 2) and PLM (Redox couple 3), respectively. It shows high redox peak current which is several times of other modified electrodes. It indicates that PLM-PNR-MWCNT-GO hybrid composite is more reversible, active and compact among these modifiers. It also proves that the immobilization of PLM and PNR can be successfully enhanced by the high conductive and high steric MWCNT-GO structure.

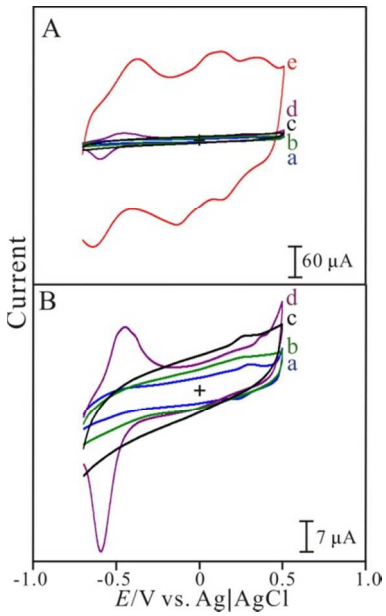

Fig. 2 (A) Cyclic voltammograms of different modifiers containing (a) PLM, (b) GO, (c) MWCNT, (d) PNR, and (e) PLM-PNR-MWCNT-GO modified GCEs examined in pH 7 PBS. (B) Scale-up voltammograms of (a) PLM, (b) GO, (c) MWCNT, and (d) PNR modified GCEs examined in pH 7 PBS. Scan rate = 0.1 Vs^{-1}.

Surface morphology of these modified electrodes was studied by SEM and AFM. Fig. S2 shows the SEM images for (A) GO, (B) MWCNT, (C) PLM, (D) PNR, (E) PLM-PNR, (F) MWCNT-GO, (G) PLM-PNR-GO, and (H) PLM-PNR-MWCNT-GO, respectively. Fig. S2A—D exhibit single materials with unique structures of plane-like clusters (GO), steric clusters (MWCNT), snowflake clusters (PLM), and globular-like clusters (PNR), respectively. Fig. S2E shows large clusters indicating the hybridization of PLM and PNR is poor and not easy to generate nanocomposite without MWCNT-GO. Fig. S2F displays the MWCNT-GO image before the hybridization of PLM and PNR polymers. It shows small clusters indicating the electrochemical reduction of GO and the adsorption of MWCNT to generate MWCNT-GO on electrode surface is successfully and compactly. Fig. S2G and H show the hybridization of PLM and PNR using GO and MWCNT-GO, respectively. By comparison, PLM-PNR-MWCNT-GO exhibits the structure of small fiber-like clusters. Considering the previous report,[50] this phenomenon can be explained by that MWCNT-GO can provide more steric structure for the hybridization of PLM and PNR. They are further considered in AFM images.

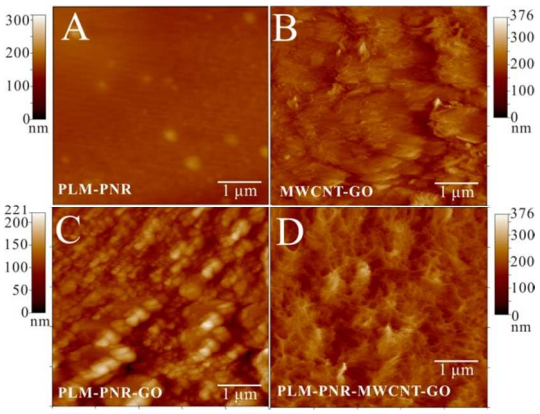

Fig. 3 AFM images of (A) PLM-PNR, (B) MWCNT-GO, (C) PLM-PNR-GO, and (D) PLM-PNR-MWCNT-GO coated ITO electrodes.

Fig. 3 shows the AFM images of (A) PLM-PNR, (B) MWCNT-GO, (C) PLM-PNR-GO, and (D) PLM-PNR-MWCNT-GO, respectively. PLM-PNR shows less clusters without obvious images might indicate the hybridization is poor to generate hybrid films when compared to PLM-PNR-GO and PLM-PNR-MWCNT-GO images. When MWCNT-GO was immobilized on electrode surface (Fig. 3B) it shows the plane-like and fiber-like structure. This phenomenon indicates that the conductive and high specific surface area can be constructed by our method. Particularly, PLM-PNR-MWCNT-GO shows specific porous mycelium-like nanostructure indicating that PLM and PNR nanofibers can be easily immobilized on MWCNT and GO due to high conductive and high specific surface area. The AFM images of these films show average diameter of 67.5 nm, 13.7 nm, 11.6 nm, and 17.8 nm for PLM-PNR, MWCNT-GO, PLM-PNR-GO, and PLM-PNR-MWCNT-GO, respectively. These modifiers are proved in nanocomposites with average roughness of 6.5 nm, 20.3 nm, 19.2 nm, and 22.6 nm, respectively. They display similar morphological properties in the results of SEM and AFM. One can conclude that the mycelium-like nanocomposite (PLM-PNR-MWCNT-GO) can be easily prepared by that using a high conductive and high specific area (MWCNT-GO) to enhance the hybridization of different polymers (PLM and PNR).

The influence of the scan rate and pH condition on PLM-PNR-MWCNT-GO/GCE electrochemical response was also studied. Fig. 4A shows the voltammograms of PLM-PNR-MWCNT-GO examined with different scan rate of 10 ─ 500 mVs^{-1}. It shows obvious three redox couples with small peak-to-peak separation and higher current response. Obvious redox couples represents that PLM-PNR-MWCNT-GO can be well immobilized on GCE and it shows stable current response in the scan rate of 10 ─ 500 mVs^{-1}. PLM-PNR-MWCNT-GO has small peak-to-peak separation indicating reversible and fast electron transfer processes. Both anodic and cathodic peak currents are directly proportional to scan rate (inset of Fig. 4A), suggesting a surface controlled process in the electrochemical system. The observation of well-defined and persistent cyclic voltammetric peaks indicates that PLM-PNR-MWCNT-GO/GCE exhibits electrochemical response characteristics of redox species confined on the electrode. The apparent surface coverage (Γ) was estimated by following equation:

$$I_p = n^2F^2\nu A\Gamma/4RT \quad (1)$$

where, I_p is the peak current of the PLM-PNR-MWCNT-GO composite electrode; n is the number of electron transfer; F is Faraday constant (96485 C mol^{-1}); ν is the scan rate ($mV\ s^{-1}$); A is the area of the electrode surface (0.07 cm^2); R is gas constant (8.314 J mol^{-1} K^{-1}); and T is the room temperature (298.15 K). Assuming a one-electron process for PLM and a two-electron process for NR and PNR in the present case, the Γ was calculated in 4.04×10^{-9} mol cm^{-2}, 1.43×10^{-9} mol cm^{-2}, and 1.36×10^{-9} mol cm^{-2} for PLM, NR, and PNR, respectively.

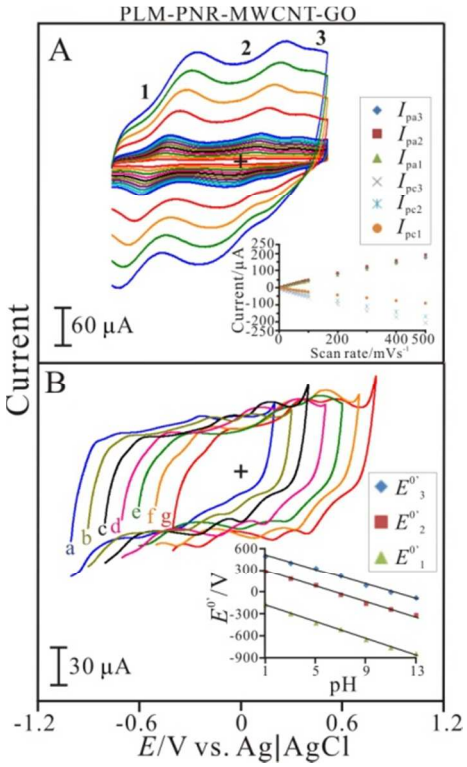

Fig. 4 Cyclic voltammograms of PLM-PNR-MWCNT-GO/GCE examined with (A) different scan rate: 10 ─ 500 mVs^{-1} (pH 7 PBS) and (B) different pH: 1 ─ 13 (scan rate = 0.1 Vs^{-1}), respectively. Insets: the plots of peak current vs. scan rate and formal potential ($E^{0'}$) vs. pH.

These values are several folds of that in previous works of PLM, NR, and PNR.[44,46,48,49] High surface coverage indicates that the hybrid composite might be compact with more electroactive species on electrode surface. One can conclude that MWCNT-GO provides more active sites to load more electroactive species. To ascertain the effect of pH, PLM-PNR-MWCNT-GO/GCE was examined in different pH solutions (pH 1 – 13). Fig. 4B presents the PLM-PNR-MWCNT-GO redox peaks which are shifted to more negative potential as increasing pH value of solution. It shows stable redox peaks in various pH conditions. This result is the same even though PLM-PNR-MWCNT-GO is repeatedly examined and change testing order of pH condition. It indicates that PLM-PNR-MWCNT-GO hybrid composite is active and

stable in wide pH condition. The characteristic PNR redox couples (with formal potential of $E^{0'}_1$ and $E^{0'}_2$) exhibit the significant slopes of -56.7 mV pH^{-1} (y = -56.7x – 127.4, R^2 = 0.997) and -51.8 mV pH^{-1} (y = -51.8x + 332.9, R^2 = 0.995) for redox couple 1 and 2, respectively. The PLM redox couple ($E^{0'}_3$) is also pH-dependent with a slope of -50.3 mV pH^{-1} (y = -50.3x + 564, R^2 = 0.995). These slopes are close to that given by the Nernstian equation, suggesting a two-electron and two-proton transfer for NR and PNR redox processes.[48,49] For PLM redox process, it is suggested as a one-electron and one-proton transfer considered with previous result.[44,46] It represents the electrochemical behaviors through the reduction and oxidation states for PLM, NR and PNR and the results are also close to previous reports.[44,46,48,49] As the result, the hybrid composites can be stable and electroactive in different pH buffer solutions.

3.2 Electrocatalysis of NADH and amperometric response at PLM-PNR-MWCNT-GO electrode

The electrocatalytic activity of the PLM-PNR-MWCNT-GO electrode towards the oxidation of NADH in pH 7 PBS was investigated by cyclic voltammetry. Fig. 5 displays the voltammograms of PLM-PNR-MWCNT-GO/GCE in pH 7 PBS with/without 5×10^{-4} M NADH. PLM-PNR-MWCNT-GO/GCE shows two obvious oxidation peaks at about +0.1 V and +0.33 V for NADH. These two characteristic oxidation peaks are related to PNR and PLM redox processes indicating that PLM and PNR are active to NADH oxidation.

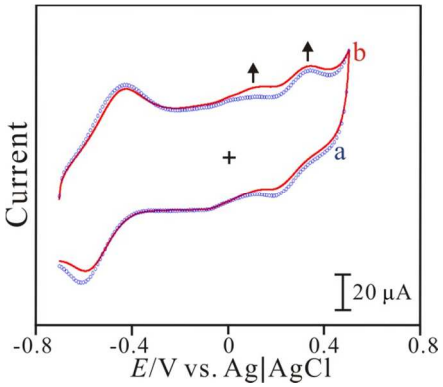

Fig. 5 Cyclic voltammograms of PLM-PNR-MWCNT-GO/GCE examined in pH 7 PBS in the (a) absence and (b) presence of 5×10^{-4} M NADH.

In order to clarify the activity of the proposed PLM-PNR-MWCNT-GO hybrid composite, different modifiers were used for electrocatalytic oxidation of NADH. Fig. S3 shows the voltammograms of (a) GCE, (b) PLM-MWCNT-GO, (c) PLM-PNR-MWCNT, (d) PLM-PNR-GO, and (e) PLM-PNR-MWCNT-GO examined in pH 7PBS containing 1×10^{-4} M NADH. The proposed composite shows much higher current response in the presence of NADH compared to other modifiers. The activities of various modifiers are further evaluated by the anodic peak potential (E_{pa}) and net current response (ΔI_{pa}) as shown in Table S1. By comparison, the anodic peaks for NADH oxidation are frequently found at about +0.15 V and +0.35 V, corresponding to our previous PLM/MWCNT system.[46] Moreover, these anodic peaks seem varying as different hybrid composites. One can see that the PLM-PNR-MWCNT-GO can provide comparable anodic peaks at +0.144 V and +0.369 V (with low overpotentail compared to bare GCE) and significant current response (ΔI_{pa2} = 18.5 μA and ΔI_{pa3} = 5.9 μA) for NADH oxidation. One can conclude that the PLM-PNR-MWCNT-GO is electroactive so that can be the candidate as a good bioelectrocatalyst for NADH sensing.

Fig. 6A shows amperometric responses of PLM-PNR-MWCNT-GO modified electrode with several additions of NADH obtained by amperometry. They were carried out with electrode rotation speed of 5000 rpm and individually applied potential at +0.1 V. PLM-PNR-MWCNT-GO/GCE shows significant amperometric responses for NADH additions spiked by micro-syringe. Inset (a) of Fig. 6A shows low detection limit of 1.33×10^{-8} M (S/N = 3) and short response time less than 10 s. Inset (b) of Fig. 6A presents the calibration curve, it provides two linear concentration ranges of 1.33×10^{-8}–1.95×10^{-4} M and 2.08×10^{-4}–5.81×10^{-4} M. The sensitivity is estimated in 288.9 μA mM^{-1} cm^{-2} and 151.3 μA mM^{-1} cm^{-2} with the regression equations of I_{NADH}(μA) = 20.4C_{NADH}(μM) + 0.1 (R^2 = 0.996) and I_{NADH}(μA) = 10.7C_{NADH}(μM) + 1.9 (R^2 = 0.995), respectively. Two linear concentration ranges might be caused by the modifier's nature. In our viewpoints, the PLM-PNR-MWCNT-GO has some kind of concentration tolerance for NADH with specific linearity in the low (1.33×10^{-8}–1.95×10^{-4} M) and high (2.08×10^{-4}–5.81×10^{-4} M) concentration ranges. Having above information, it would be easier to compensate the electronic signal of NADH sensor for practical fabrication.

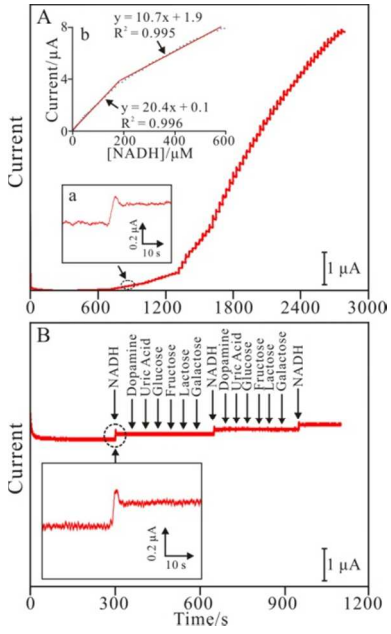

Fig. 6 Amperograms of PLM-PNR-MWCNT-GO/GCE examined in pH 7 PBS containing (A) [NADH] = 1.33×10^{-8} – 5.94×10^{-4} M and (B) potential interferants: dopamine, uric acid, glucose, fructose, lactose, galactose (1.33×10^{-5} M for each addition). Insets are the scale-up amperomogram and the calibration curve.

Table 1 presents the main performances of published data about NADH sensors based on different modified materials. It shows competitive performance in the literature. By comparison, the NADH sensor presented in this paper exhibits one of the

highest sensitivity with low detection limit and low overpotential. A significant lower detection limit and a higher sensitivity were reported for sensors based on MWCNT. It might be caused by the synergistic effect of obtained CNTs/conducting polymer possess properties of the individual components similar to previous reports.[18-23]

One can conclude that the active hybrid composite shows competitive performance to other materials (Table 1). It has the excellent ability to determine NADH due to low detection limit, low working potential, and high current response, suggesting as a high sensitive NADH sensor.

Table 1. Performance for sensing NADH with various materials modified electrodes.

Modified materials	$E_{app.}$[a] (V) vs. Ag/AgCl	LOD[b] (μM)	Sensitivity (μA mM^{-1} cm^{-2})	Ref.
polyluminol/MWCNT	0.10	0.6	183.9	[46]
PNR-FAD	0.10	10	21.5	[49]
Highly ordered mesoporous carbon	0.25	1.61	93	[51]
Chemically reduced graphene oxide	0.45	10	2.68	[52]
Graphite/PMMA	0.45	3.5	68	[53]
MWCNT/poly-Xa	0.45	0.1	2.2	[54]
ERGO-PTH/GC	0.40	0.1	143	[55]
poly-Xa/FAD/MWCNT	0.15	171	155	[56]
PAH/SPE	0.60	0.22	125.9	[57]
PLM-PNR-MWCNT-GO	0.1	0.0133	288.9	This work

[a] $E_{app.}$ = Applied potential.

[b] LOD = Limit of detection.

3.3 Interference study of the PLM-PNR-MWCNT-GO composite

The PLM-PNR-MWCNT-GO modified electrode was studied with the interference effect on amperometric response for NADH. It was examined in the presence of several interferants including ascorbic acid, dopamine, uric acid, glucose, fructose, lactose, and galactose ($E_{app.}$ = +0.1 V). Fig. 6B shows the amperometric response of PLM-PNR-MWCNT-GO with various interferants. No interference occurred in the amperograms except of the case of ascorbic acid. It was further applied to study the correlation between current response and potential compared to bare electrode by linear sweep voltammetry (LSV). Fig. S4A shows the LSV voltammograms of PLM-PNR-MWCNT-GO examined in the presence of ascorbic acid and NADH. It shows similar oxidation peaks for ascorbic acid and NADH so that it is further considered using a bare electrode. Fig. S4B shows the LSV voltammograms of bare electrode examined in the presence of ascorbic acid, NADH, and their mixture. Inset of Fig. S4B presents the relationship between peak current and species. Good correlation is found at +0.45 V, it is noticed that the current response of AA+NADH mixture is almost two times of AA. This information indicates that NADH can be determined more exactly by inspection of ascorbic acid using a bare electrode. This phenomenology might be explained by the overpotential of AA and NADH. In our viewpoint, a bare GCE can show different anodic peaks at +0.2 V and +0.45 V, corresponding to their overpoentials for AA and NADH, respectively. Here we have two conclusions: (i) one might gain the accumulated current response in the voltammograms after scanning cross the overptential of all electroactive analytes; (ii) the accumulated current responses at +0.2 V and +0.45 V might provide the information about NADH/AA ratio in the mixture. One can conclude that the modified electrode can avoid interference from most of interferants to be a good electrocatalyst to determine NADH.

3.4 Stability study of the PLM-PNR-MWCNT-GO modified electrodes

The reproducibility and stability of the sensor were evaluated. Five PLM-PNR-MWCNT-GO electrodes were investigated at +0.1 V to compare their amperometric current responses. Ten successive measurements of NADH on one PLM-PNR-MWCNT-GO electrode yielded an R.S.D. of 2.1%, indicating that the sensor was stable and highly reproducible. The long-term stability of the sensor was also evaluated by measuring its current response to NADH within a 7-day period. The sensor was stored at 4 □ and its sensitivity was tested every day. The current response of PLM-PNR-MWCNT-GO electrode was approximately 93% of its original counterpart, which can be mainly attributed to the chemical stability of PLM and PNR on MWCNT-GO.

4. Conclusions

PLM and PNR hybrid films can be successfully prepared on electrode surface and further enhanced by MWCNT-GO. PLM-PNR-MWCNT-GO shows specific mycelium-like nanostructure indicating that PLM and PNR nanofibers can be easily immobilized on MWCNT and GO due to high conductive and high specific surface area. The modified electrode is electrochemically characterized and examined as a novel NADH sensor, which presents attractive analytical features such as high sensitivity, low overpotential, low detection limit, good stability, and good reproducibility.

Acknowledgements

We acknowledge National Science Council (project no. NSC1012113M027001MY3), Taiwan.

Notes and references

Electroanalysis and Bioelectrochemistry Lab, Department of Chemical Engineering and Biotechnology, National Taipei University of Technology, No.1, Section 3, Chung-Hsiao East Road, Taipei 106,

Taiwan. Fax: (886)-2-27025238; Tel: (886)-2-27017147; E-mail: smchen78@ms15.hinet.net

† Electronic Supplementary Information (ESI) available: [details of any supplementary information available should be included here]. See DOI: 10.1039/b000000x/

‡ Footnotes should appear here. These might include comments relevant to but not central to the matter under discussion, limited experimental and spectral data, and crystallographic data.

1 L. Gorton and E. Dominguez, *Electrochemistry of NAD(P)$^+$/NAD(P)H in Encyclopedia of Electrochemistry*, Wiley-VCH, Weinheim, 2002, **9**, 67–143.

2 S. Liu, Z. Du, P. Li and F. Li, *Biosensors and Bioelectronics*, 2012, **35**, 443–446.

3 Y.P. Hung, J.G. Albeck, M. Tantama and G. Yellen, *Cell Metabolism*, 2011, **14**, 545–554.

4 W.D. Koning and K.V. Dam, *Analytical Biochemistry*, 1992, **204**, 118–123.

5 K. Yamada, N. Hara and T. Shibata, *Analytical Biochemistry*, 2006, **352**, 282–285.

6 F. Sadanaga-Akiyoshi, H. Yao and S. Tanuma, *Neurochemical Research*, 2003, **28**, 1227–1234.

7 W.J. Xie, A.S. Xu and E.S. Yeung, *Analytical Chemistry*, 2009, **81**, 1280–1284.

8 H. Yao, H.B. Halsall, W.R. Heineman and S.H. Jenkins, *Clinical Chemistry*, 1995, **41**, 591–598.

9 X. He, X. Ni, Y. Wang, K. Wang, L. Jian, *Talanta*, 2011, **83**, 937–942.

10 A. Bergel, J. Souppe and M. Comtat, *Analytical Biochemistry*, 1989, **179**, 382–388.

11 Y. Yan, W. Zheng, L. Su and L. Mao, *Advanced Materials*, 2006, **18**, 2639–2643.

12 A. Radoi and D. Compagnone, *Bioelectrochemistry*, 2009, **76**, 126–134.

13 J. Moiroux and P.J. Elving, *Analytical Chemistry*, 1978, **50**, 1056–1062.

14 Z. Samec and P.J. Elving, *Journal of Electroanalytical Chemistry*, 1983, **144**, 217–234.

15 W.J. Blaedel and R.A. Jenkins, *Analytical Chemistry*, 1975, **47**, 1337–1343.

16 M. Musameh, J. Wang, A. Merkoci and Y. Lin, *Electrochemistry Communications*, 2002, **4**, 743–746.

17 M.G. Zhang, A. Smith and W. Corski, *Analytical Chemistry*, 2004, **76**, 5045–5050.

18 C. Deng, J. Chen, X. Chen, C. Xiao, Z. Nie and S. Yao, *Electrochemistry Communications*, 2008, **10**, 907–909.

19 R.H. Baughman, A.A. Zakhidov and W.A.D. Heer, *Science*, 2002, **297**, 787–792.

20 P.R. Lima, W.D.J.R. Santos, A.B. Oliveira, M.O.F. Goulart and L.T. Kubota, *Biosensors and Bioelectronics*, 2008, **24**, 448–454.

21 S. Hrapovic, Y. Liu, K.B. Male and J.H.T. Luong, *Analytical Chemistry*, 2004, **76**, 1083–1088.

22 J. Sandler, M. Schaffer, T. Prasse, W. Bauhofer, K. Schulte and A.H. Windle, *Polymer*, 1999, **40**, 5967–5971.

23 C.Y. Wei, D. Srivastava and K.J. Cho, *Nano Letters*, 2002, **2**, 647–650.

24 M.G. Hughes, Z. Chen, M.S.P. Schaffer, D.J. Fray and A.H. Windle, *Chemistry of Materials*, 2002, **14**, 1610–1613.

25 K.H. An, S.Y. Jeong, H.R. Hwang and Y.H. Lee, *Advanced Materials*, 2004, **16**, 1005–1009.

26 E. Kymakis and G.A.J. Amaratunga, *Applied Physics Letters*, 2002, **80**, 112–114.

27 H.S. Woo, R. Czerw, S. Webster, D.L. Carroll, J.W. Park and J.H. Lee, *Synthetic Metals*, 2001, **116**, 369–372.

28 I. Musa, M. Baxendale, G.A.J. Amaratunga and W. Eccleston, *Synthetic Metals*, 1999, **102**, 1250–1254.

29 J.N. Coleman, S. Curran, A.B. Dalton, A.P. Davey, B. McCarthy, W. Blau and R.C. Barklie, *Synthetic Metals*, 1999, **102**, 1174–1175.

30 A.K. Geim and K.S. Novoselov, *Nature Materials*, 2007, **6**, 183–191.

31 J.M. Parpia, H.G. Craighead and P.L. McEuen, *Science*, 2007, **315**, 490–493.

32 S. Gilje, S. Han, M. Wang, K.L. Wang and R.B. Kaner, *Nano Letters*, 2007, **7**, 3394–3398.

33 F. Schedin, A.K. Geim, S.V. Morozov, E.W. Hill, P. Blake, M.I. Katsnelson and K.S. Novoselov, *Nature Materials*, 2007, **6**, 652–655.

34 V.C. Tung, J.H. Huang, I. Tevis, F. Kim, J. Kim, C.W. Chu, S.I. Stupp and J.X. Huang, *Journal of the American Chemical Society*, 2011, **133**, 4940–4947.

35 J.H. Huang, J.H. Fang, C.C. Liu and C.W. Chu, *ACS Nano*, 2010, **5**, 6262–6271.

36 C. Deng, F. Qu, H. Lu and M. Yang, *Biosensors and Bioelectronics*, 2011, **26**, 4810–4814.

37 S. Ge, M. Yan, J. Lu, M. Zhang, F. Yu, J. Yu, X. Song and S. Yu, *Biosensors and Bioelectronics*, 2012, **31**, 49–54.

38 T.Y. Huang, J.H. Huang, H.Y. Wei, K.C. Ho and C.W. Chu, *Biosensors and Bioelectronics*, 2013, **43**, 173–179.

39 S. He, W. Shi, X. Zhang, J. Li and Y. Huang, *Talanta*, 2010, **82**, 377-383.

40 J. Rong, Y. Chi, Y. Zhang, L. Chen and G. Chen, *Electrochemistry Communications*, 2010, **12**, 270–273.

41 X.M. Chen, B.Y. Su, X.H. Song, Q.A. Chen, X. Chen and X.R. Wang, *Trends in Analytical Chemistry*, 2011, **30**, 665–676.

42 X. Yang, Y. Guo and A. Wang, *Analytica Chimica Acta*, 2010, **666**, 91–96.

43 D. Tian, C. Duan, W. Wang and H. Cui, *Biosensors and Bioelectronics*, 2010, **25**, 2290–2295.

44 S.M. Chen and K.C. Lin, *Journal of Electroanalytical Chemistry*, 2002, **523**, 93–105.

45 K.C. Lin and S.M. Chen, *Journal of Electroanalytical Chemistry*, 2006, **589**, 52–59.

46 K.C. Lin, C.Y. Yin and S.M. Chen, *Analyst*, 2012, **137**, 1378–1383.

47 A.A. Karyakin, E.E. Karyakina and H.L. Schmidt, *Electroanalysis*, 1999, **11**, 149–155.

48 S.M. Chen and K.C. Lin, *Journal of Electroanalytical Chemistry*, 2001, **511**, 101–114.

49 K.C. Lin, Y.C. Lin and S.M. Chen, *Analyst*, 2012, **137**, 186–194.

50 Q. Zhang, S. Yang, J. Zhang, L. Zhang, P. Kang, J. Li, J. Xu, H. Zhou and X.M. Song, *Nanotechnology*, 2011, **22**, 494010 (7pp).

51 M. Zhou, L. Shang, B. Li, L. Huang and S. Dong, *Electrochemistry Communications*, 2008, **10**, 859–863.

52 M. Zhou, Y. Zhai and S. Dong, *Analytical Chemistry*, 2009, **81**, 5603–5613.

53 H. Dai, H. Xu, Y. Lin, X. Wu and G. Chen, *Electrochemistry Communications*, 2009, **11**, 343–346.

54 F.D.A.D.S. Silva, C.B. Lopes, E.D.O. Costa, P.R. Lima, L.T. Kubota and M.O.F. Goulart, *Electrochemistry Communications*, 2010, **12**, 450–454.

55 Z. Li, Y. Huang, L. Chen, X. Qin, Z. Huang, Y. Zhou, Y. Meng, J. Li, S. Huang, Y. Liu, W. Wang, Q. Xie and S. Yao, *Sensors and Actuators B*, 2013, **181**, 280–287.

56 K.C. Lin, Y.S. Li and S.M. Chen, *Sensors and Actuators B*, 2013, **184**, 212–219.

57 L. Rotariu, O.M. Istrate and C. Bala, *Sensors and Actuators B*, 2014, **191**, 491–497.